The Effect of Thermal Annealing Processes on Graphene

K. Kumar, Y.-S. Kim, Y. Tian, X. Li, A. Pallikaras, E.H. Yang

Dept. of Mechanical Engineering, Stevens Institute of Technology
Castle Point-on-Hudson, Hoboken, NJ 07030, USA, eyang@stevens.edu

ABSTRACT

We present an in-depth investigation of the consequence of gas and vacuum annealing utilized to remove polymer (PMMA) residues on the electronic doping, strain, and morphology of chemical vapor deposition grown graphene. We demonstrate that annealing under gas or vacuum increases doping levels in graphene as residual PMMA is burned off, interfacial water is evaporated, and graphene conformally contacts the substrate. This is corroborated by AFM measurements, indicating a need for further research on graphene transfer or growth methods where substrate-induced doping is minimized. These results are significant for determining the extent of PMMA influence on graphene during the transfer process and/or device fabrication.

Keywords: graphene, annealing, chemical vapor deposition, Raman spectroscopy, atomic force microscopy

1 INTRODUCTION

Graphene has generated interest in the research community because of its many applications. For utilization in devices, graphene must be transferred to an insulating substrate and patterned into the desired shape. Fig. 1 illustrates a common methodology for chemical vapor deposition (CVD)-grown graphene transfer. Poly(methyl methacrylate) (PMMA) is spin-coated on the graphene; after etching the growth catalyst, the PMMA-graphene stack is rinsed in DI water and placed on the desired substrate. At this point, the PMMA is removed with an organic solvent and thermal annealing removes most post-solvent residue. Additionally, to fabricate CVD graphene devices, PMMA or similar polymer may be re-introduced as a lithography mask. In both cases, graphene is exposed to PMMA, which must be removed. It is well known that solvent rinses leave a layer of polymer residue and that these can be largely removed by thermal annealing in gaseous atmospheres such as Ar, H_2, H_2/Ar, N_2, or vacuum. Current annealing is also explored as a route to remove polymeric contaminants, but can only be performed after electrodes have been fabricated on the graphene. On the other hand, thermal annealing can be performed at any step in the device fabrication process, from immediately after transfer to the substrate or immediately after device fabrication [1], [2]. Therefore, this work provides a more complete understanding of thermal annealing processes by comparing the effects of alternating hydrogen and ambient (oxygen) annealing with the effects of vacuum annealing on graphene Raman spectra and sample topography. These results are of importance to researchers utilizing thermal annealing to remove residues graphene for devices where the electronic and mechanical performance of the graphene is critical.

2 EXPERIMENTAL METHODS

The CVD graphene samples employed in this work were grown at atmospheric pressure on 25 mm thick Cu foils (Alfa Aesar, 99.999% purity) in a quartz tube furnace at 1000°C with 1000 sccm of Argon, 30-50 sccm of H_2 and 10 sccm of CH_4 flowing during growth. The graphene transfer process was as follows. Each sample was cut in half, where the first half was placed directly in citric acid etchant (hereafter referred to as NP for No PMMA exposure), and the second half (P, for PMMA exposed) was spin-coated with a 495,000 molecular weight PMMA (Sigma-Aldrich) dissolved in anisole at a spin speed of 4000 rpm for 1 min followed by 1000 rpm for 1 min (acceleration of 1000 rpm/s). The resulting PMMA thickness was approximately 50 nm. The sample was then dried at 25°C in laboratory ambient air for 12 hrs after which it was placed in an etchant bath. For both P and NP samples, the Cu foil was etched for approximately 12 hrs and then etched for an additional 24-30 hrss in a fresh citric acid bath to ensure the complete removal of Cu. The samples were placed in two successive water baths of 12 hrs each and then transferred to a 90 nm SiO_2/Si substrate. After being allowed to dry in laboratory ambient air, the P samples were placed in an acetone bath at room temperature overnight followed by an acetone bath at 55C for 2 hrs to ensure an effective PMMA removal. The transferred P and NP samples were then either subjected to annealing in H_2/Ar atmosphere at 350C for 2 hrs followed by annealing in ambient atmosphere at 350C for 2 hrs or vacuum annealing at 350C for 2 hrs.

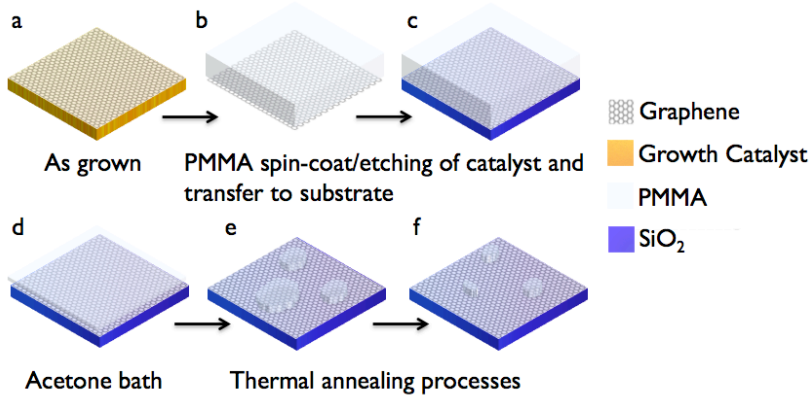

Figure 1: Schematic illustrating graphene transfer and PMMA clean. a) As grown graphene is (b) spin-coated with a layer of PMMA, growth metal catalyst is etched and PMMA/graphene stack is washed in DI water and (c) transferred to desired substrate. (d) The sample is given an acetone bath, which leaves a layer of PMMA residue. This residue is burned off in various thermal annealing steps (e,f).

3 RESULTS

3.1 Annealing under gaseous atmosphere

Fig. 2 details Raman peak parameter changes in graphene due to H_2/Ar annealing followed by ambient annealing. Of immediate note is the drastic broadening and substantial stiffening of all peaks after H_2/Ar annealing. The representative spectra show a broad fluorescent signal from 1200 to 1650 cm^{-1} superimposed upon the greatly broadened D and G peaks and the suppressed G' peak after the H_2/Ar anneal for both P and NP graphene. This signal is partially attributed to the existence of amorphous carbon (mixture of sp^2- and sp^3-bonded carbon) from the scission of PMMA. Indeed, in [2], it is reported that a similar signal arises when PMMA-transferred graphene is suspended, and is dampened after several H_2/Ar and ambient anneals, as the PMMA is removed. However, here we see this signal arise in graphene transferred *both with and without PMMA* post-H_2/Ar anneal. Therefore, we attribute the fluorescence and increased disorder to the functionalization of graphene with H atoms and other contaminants forming sp^3 sites during the annealing process [3]. This sp^3 functionalization is known to superimpose a strong fluorescent peak in carbon with high hydrogen content.

Subsequently, upon ambient annealing, we find that the fluorescent signal largely disappeared and $I_{G'}/I_G$ returned to its original values. However, the samples are now highly hole-doped as evidenced by the G' and G band stiffening compared to the as-transferred positions. Interestingly, the P Γ_D and ω_D largely returned to the as transferred values of ~24 cm^{-1} and ~1345 cm^{-1} with I_D/I_G also returning to very close to as transferred values, pointing to removal of both PMMA residue and H-functionalized sp^3 sites.

3.2 Annealing under vacuum atmosphere

Vacuum annealing of graphene is expected to desorb PMMA residues and other atmospheric contaminants. This would result in a softening of $\omega_{G'}$ and ω_G as hole dopants are removed, which would be observed if the Raman spectra of the samples were measured in vacuum. However, upon exposure to atmospheric conditions after the vacuum annealing, the G and G' bands (i.e., post-annealing values) would stiffen compared to pre-annealing values. This change is not clearly observed in our experiments from the post-anneal values (Fig. 3); the G band positions, especially being more sensitive to charge doping, are almost the same as the as-transferred values and largely within variation of spectral values. Several processes could account for this effect. Initially, the removal of PMMA would reduce hole doping, but uncover sites where atmospheric H_2O or O_2 could adsorb and then increase hole doping. Next, any thermal annealing process removes the interfacial water layer between the graphene and substrate, decreasing H_2O-assisted hole doping and thus brings the graphene layer closer to the substrate, increasing n-type charge injection from the substrate [4]. As the graphene layer conformably contacts the corrugated SiO_2, the distortion of the lattice would relax short range C-C bonds and allow increased chemical reactivity, especially in the grain boundaries, to adsorbates such as atmospheric hole dopants. Overall, the net effect would be to maintain charge doping in the graphene layer as we discern above. Any minor strain effects from the conformal SiO_2 contact with P graphene (stiffened G' and softened G with compressive strain) would then be overwhelmed by the shifts from doping.

3.3 Annealing under vacuum atmosphere

AFM measurements confirm many of these processes (Fig. 4). In the case of gaseous annealing (Fig. 4a), the existence of an amorphous carbon layer is confimed by the increase in step height from approx. 1.5 nm to 4.5 nm. This is clearly removed after ambient annealing and the layer step height is reduced to less than 1 nm as interfacial water is removed and the graphene is brought in closer contact with the substrate.

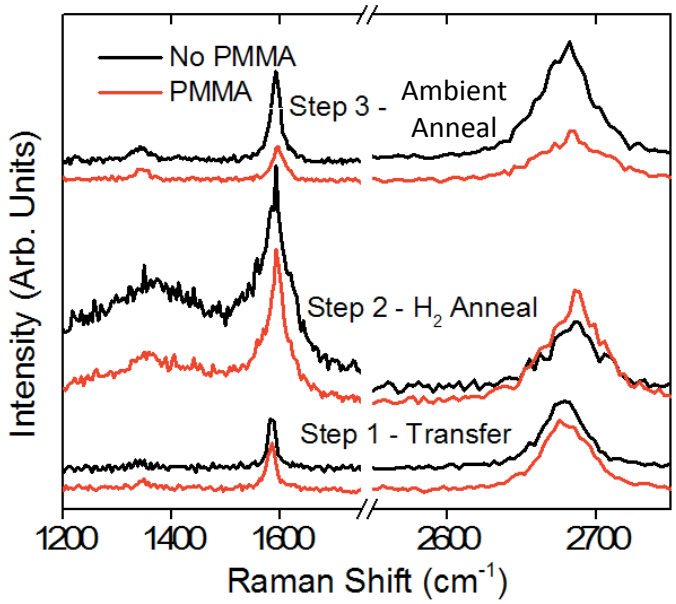

Figure 2: Raman spectra of graphene annealed under H2/Ar gas and ambient. (a) Variation in spectra of CVD graphene transferred with (red) and without (black) PMMA.

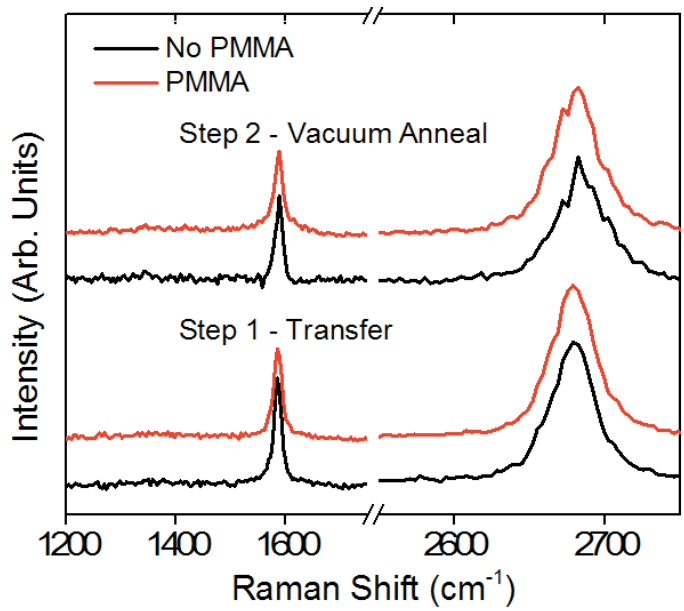

Figure 3: Raman spectra of graphene annealed under vacuum. (a) Variation in spectra of CVD graphene transferred with (red) and without (black) PMMA.

In the case of vacuum annealing (Fig. 4b), we can clearly see PMMA burned away as evidenced by the decreased step heights, bringing the CVD graphene into particularly close conformal contact with the substrate.

4 CONCLUSIONS

The important processes affecting the Raman spectra are removal and re-adsorption of surface contaminants, removal of the interfacial water layer, increased reactivity of graphene due to closer conformal contact, and minor charge injection from substrate. The stiffening of the G peak and decrease of $I_{G'}/I_G$ in the NP graphene are consistent with an increase in hole doping, although the greater increase of G' peak position signifies the effect of compressive strain. Here, the G peak position stiffening from hole doping would be in competition from the softening which would occur under this compressive strain. The $\Delta\omega_{G'}/\Delta\omega_G$ is also indicative of compressive strain from thermal cycling. However, if this compressive strain also exists in the P graphene samples after the thermal cycling, its effects could be neutralized in the Raman spectra from the influence of charge doping as mentioned above or from smaller localized deformation. We also note that $I_{G'}/I_G$ increased and I_D/I_G decreased for all P graphene consistent with theremoval of polymeric functional groups, however, the increase in Γ_D of the P graphene is not consistent with this removal. A more detailed study of the effect of annealing on sheet disorder needs to be performed in the future to elucidate such inconsistencies.

We have systematically investigated the effects of thermal annealing under gas and vacuum on the removal of PMMA and graphene properties. We utilized a combination of Raman spectroscopy and AFM to show that, while both gas and vacuum annealing techniques are effective at removing PMMA, annealing in gas introduces partially irreversible changes in the doping levels of CVD graphene from polymer residue/H-functionalization. Vacuum annealing maintained the integrity of the Raman signatures and removed most PMMA residue, despite doping induced spectral changes, making it an attractive alternative to gas annealing. Finally, analysis from step height and roughness measurements from AFM aided in the formation of a broad picture of those annealing-based processes, including removal of the interfacial graphene-substrate water layer, atmospheric doping effects, and deformation of the graphene layer, which create morphological changes and directly influence doping and strain, through removal of PMMA.

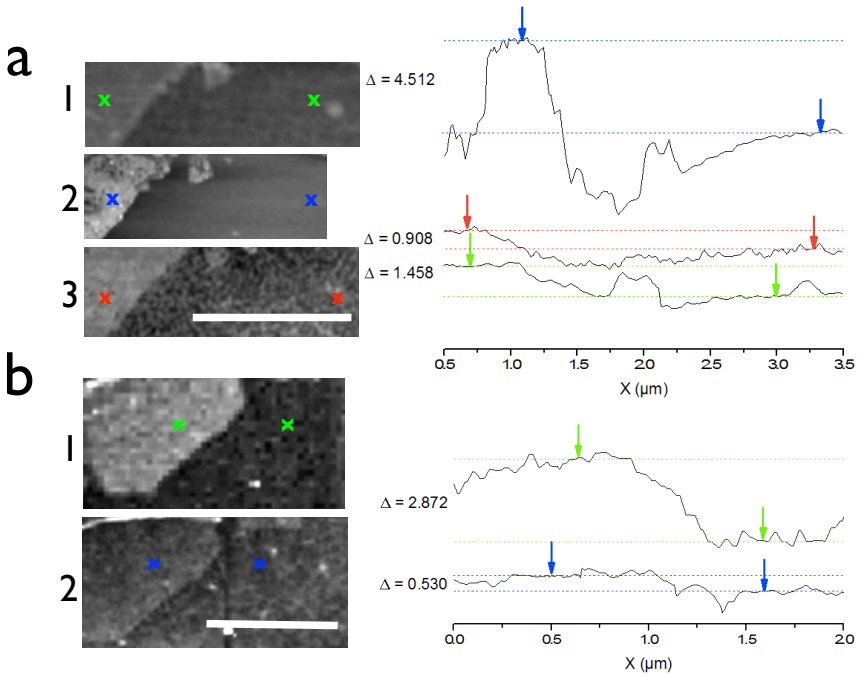

Figure 4: AFM topography scans of graphene subjected to (a) H2/Ar anneal (2) followed by ambient anneal (3) and (b) vacuum anneal. Amorphous PMMA residue increases thickness after H2/Ar anneal (right, blue arrows) and is removed after the ambient anneal (right, red arrows). After vacuum annealing (b, right) the step height measurement of 0.53 nm indicates that PMMA is almost completely removed.

5 ACKNOWLEDGEMENT

This work has been supported in part by the National Science Foundation (EECS-1040007, ECCS-1104870, ECCS-1202269 and EEC-1138244) and Air Force Office for Scientific Research (FA9550-11-1-0272, FA9550-12-1-0326).

REFERENCES

[1] J. Chan, A. Venugopal, A. Pirkle, S. McDonnell, D. Hinojos, C. W. Magnuson, R. S. Ruoff, L. Colombo, R. M. Wallace, and E. M. Vogel, "Reducing Extrinsic Performance-Limiting Factors in Graphene Grown by Chemical Vapor Deposition," *ACS Nano,* vol. 6, no. 4, pp. 3224–3229, Mar. 2012.

[2] Y.-C. Lin, C. Jin, J.-C. Lee, S.-F. Jen, K. Suenaga, and P.-W. Chiu, "Clean Transfer of Graphene for Isolation and Suspension," *ACS Nano,* vol. 5, no. 3, pp. 2362–2368, Mar. 2011.

[3] S. Ryu, M. Y. Han, J. Maultzsch, T. F. Heinz, P. Kim, M. L. Steigerwald, and L. E. Brus, "Reversible Basal Plane Hydrogenation of Graphene," *Nano Letters,* vol. 8, no. 12, pp. 4597–4602, Dec. 2008.

[4] Z. Cheng, Q. Zhou, C. Wang, Q. Li, C. Wang, and Y. Fang, "Toward Intrinsic Graphene Surfaces: A Systematic Study on Thermal Annealing and Wet-Chemical Treatment of SiO 2-Supported Graphene Devices," *Nano Letters,* vol. 11, no. 2, pp. 767–771, Feb. 2011.